

Figure S1: Generation of exosome captured *miR-26a* with *MSTP* surface peptide:

The *Lamp2b-MSTP* vector was transfected into satellite cells using Effectene (Qiagen, Valencia, CA, USA). After 6 hours of transfection, the cells were transduced with Ad-*miR-26a* (adenovirus containing *miR-26a*) or Ad-empty (control virus) in the medium containing 2% extracellular vesicle free serum (EVFS). Fresh EVFS medium was changed after 24 hours. The cells were cultured for an additional 48 hours to allow exosome release into the medium. The exosomes that are enriched with *miR-26a* (Exo/*miR-26a*) or control (Exo/ctrl) were harvested from culture medium. The size and concentration of exosomes isolated from the cultured medium of satellite cell. NanoSight Instrument was used to measure the exosome size (X axis, nanometer diameter) and concentration (Y axis, 1×10^{15} Particles / ml) in left graph. The bar graphs showed the size (middle) and concentration (right) of the exosomes isolated from cultured medium (Bars: mean \pm s.d.; n=6/group).

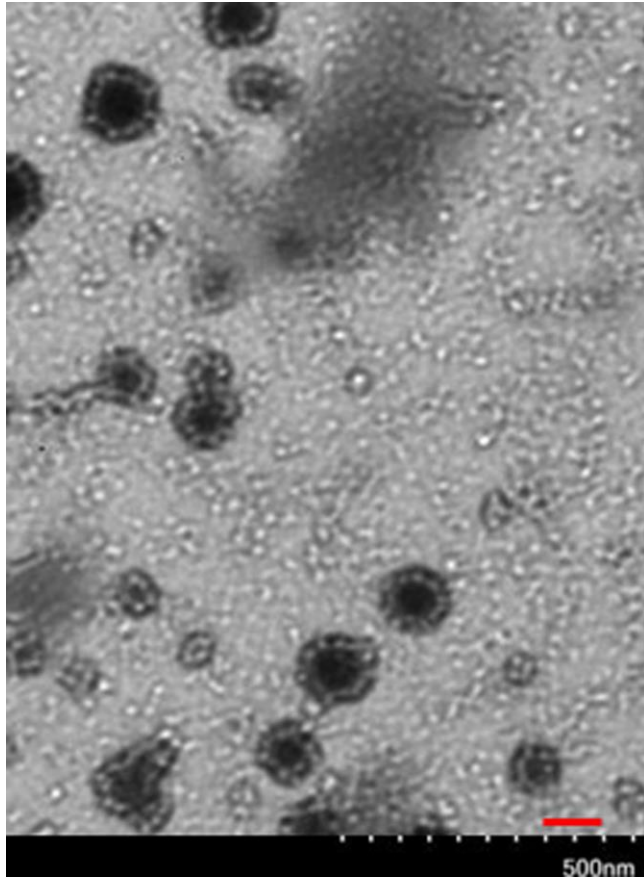


Figure S2: Exosome image taken by electron-microscope. The red scale bar indicated 100nm.

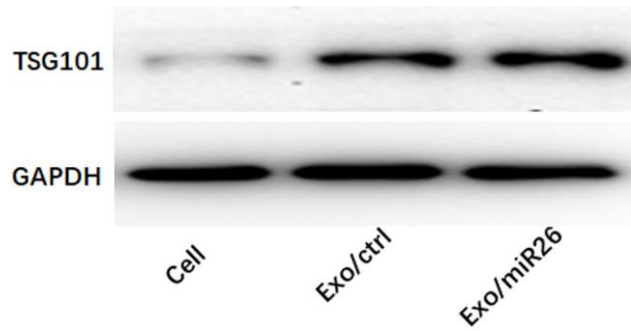


Figure S3: Generation of exosome captured *miR-26a* with *MSTP* surface peptide:

The Lamp2b-MSTP vector was transfected into satellite cells using Effectene (Qiagen, Valencia, CA, USA). After 6 hours of transfection, the cells were transduced with Ad-miR-26a (adenovirus containing miR-26a) or Ad-empty (control virus) in the medium containing 2% extracellular vesicle free serum (EVFS). Fresh EVFS medium was changed after 24 hours. The cells were cultured for an additional 48 hours to allow exosome release into the medium. The exosomes that are enriched with miR-26a (Exo/*miR-26a*) or control (Exo/ctrl) were harvested from culture medium. The proteins from cultured satellite cells and exosome isolated from conditional medium were used to detect exosome maker protein, TSG101. The Western blot showed TSG101 abundance from cells, exosome isolated from the conditional medium with control adenovirus (Exo/ctrl) and with Ad-miR-26a (Exo/*miR-26a*).

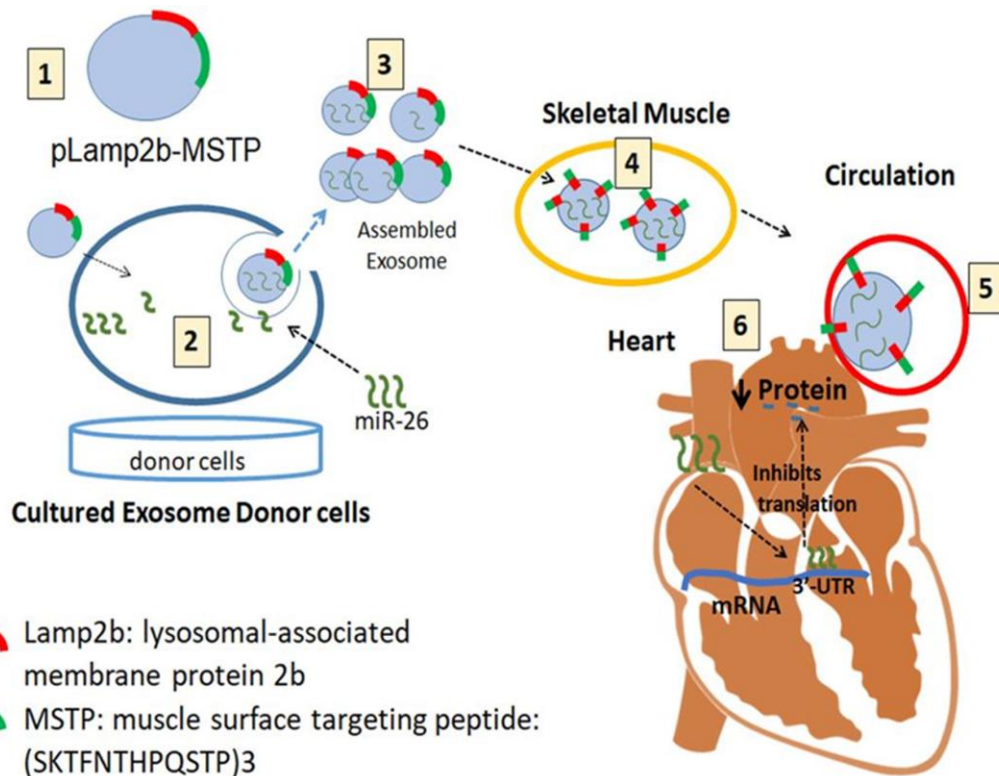


Figure S4: Generation of exosome captured *miR-26a* with MSTP surface peptide:

First, we created a vector which produces *Lamp2b* (lysosomal-associated membrane protein 2b) fused with the muscle specific surface peptide (*SKTFNTHPQSTP*)³ (#1 in Figure S4). An exosome with this peptide will target to skeletal and heart. Second, we co-transfected this vector, along with *miR-26a*, into donor cells (#2 in Figure S4). The exosomes produced from these cells contain *miR-26a* and will tend to go to muscle. Third, we collected the targeting exosomes with their miR cargo that were secreted into the conditioned medium by the donor cells (#3 in Figure S4). Fourth, we injected the exosome/miR into skeletal muscle of CKD mice (#4 in Figure S4). Fifth, muscle releases Exo/miR into the circulation (#5 in Figure S4). Because *Lamp2b* is ubiquitously expressed on the surface of exosomes, it can bring the targeting peptides (*SKTFNTHPQSTP*)³ to the exosomes surface and endow exosome-encapsulated *miR-26a* with targeting ability (#6 in Figure S4).

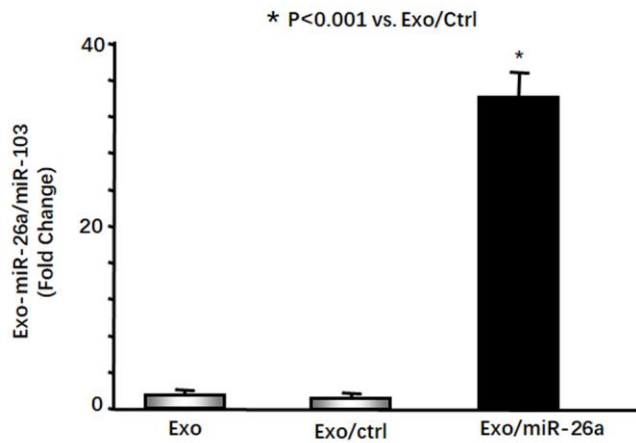


Figure S5: Generation of exosome captured *miR-26a* with MSTP surface peptide:

The exosomes that are enriched with *miR-26a* (Exo/*miR-26a*) or control (Exo/ctrl) were harvested from culture medium. RNA was isolated from exosomes of conditional medium without transfected *Lamp2b* (Exo), transfected with *Lamp2b* plus Ad-empty (Exo/Ctrl) or plus Ad-*miR-26a* (Exo/*miR-26a*). The expression of *miR-26a* was assayed by real time qPCR. The bar graph shows *miR-26a* expression from each group compared with Exo, represented by 1-fold. Results are normalized to *miR103a*. (Bars: mean \pm s.e.; n=6/group; *=p<0.05 vs. Exo/ctrl).

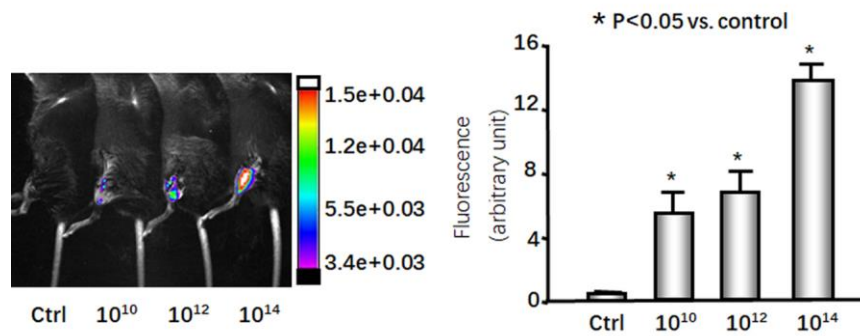


Figure S6: Generation of exosome captured *miR-26a* with *MSTP* surface peptide:

Exosome was labeled with with 1 $\mu\text{mol/l}$ fluorescent lipophilic tracer DiR. Mice were injected in the left tibialis anterior (TA) muscle with different dose of Exo/*miR-26a*. The fluorescence was assessed at 7 days after injection. The control was no injection. Representative fluorescent muscle images and intensity measurement were acquired by a Bruker Small Animal Optical Imaging System. The bright white color indicates that the signal intensity exceeded the linear signal limit. The bar graph shows fluorescence intensity from the each TA muscle. (Bars: mean \pm s.e.; n=3/group; * = p<0.05 vs. control).

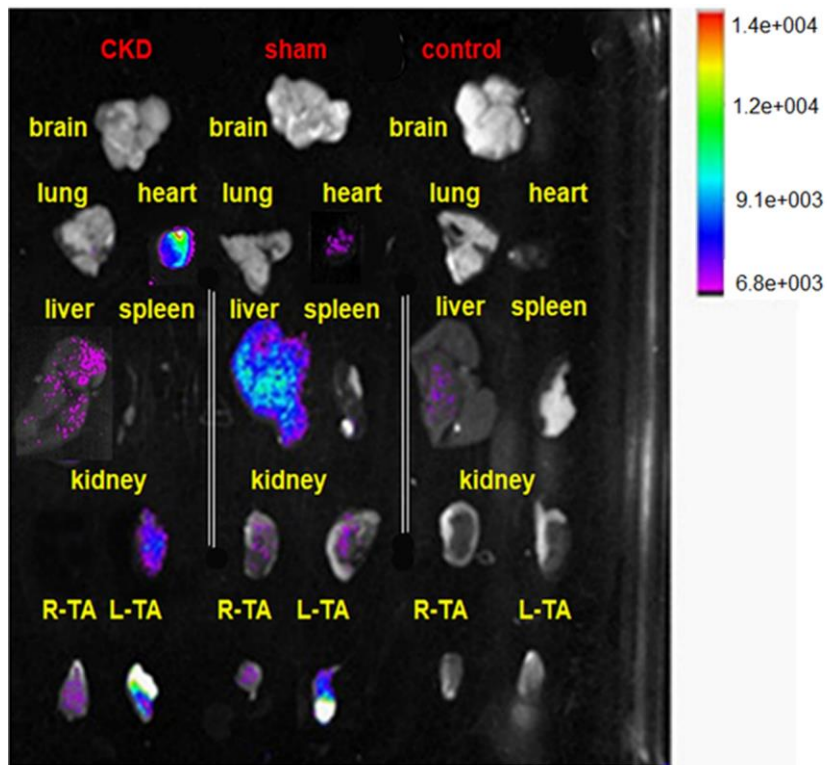


Figure S7. *miR-26a* was increased in the heart of mice with intramuscular injection of Exo/*miR-26a*

Fluorescent organ images were acquired using a Bruker Small Animal Optical Imaging System. Normal mice (right) without any injection for control, sham mice (middle) and CKD mice (left) were injected Exo/*miR-26a* labeled with 1 $\mu\text{mol/l}$ fluorescent lipophilic tracer DiR in the left TA muscle. The fluorescence was assessed at 7 days after injection.

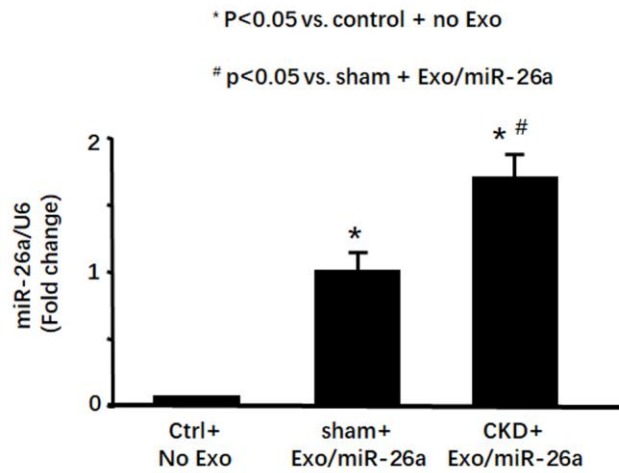


Figure S8: the expression of *miR-26a* has higher expression in CKD heart than the heart from sham operated mice after intramuscular injection of Exo/*miR-26a*

Total RNA was isolated from the heart of normal mice without exosome injection (Ctrl+no Exo), sham plus Exo/*miR-26a* and CKD plus Exo/*miR-26a* mice. The expression of *miR-26a* was assayed by real time qPCR. The bar graph shows *miR-26a* expression from sham or CKD compared with levels in control heart (represented at 1-fold). Results are normalized to *U6*. (Bars: mean \pm s.e.; n = 6/group; * = p<0.05 vs. Ctrl+no Exo, # = p<0.05 vs. sham with Exo/ctrl).

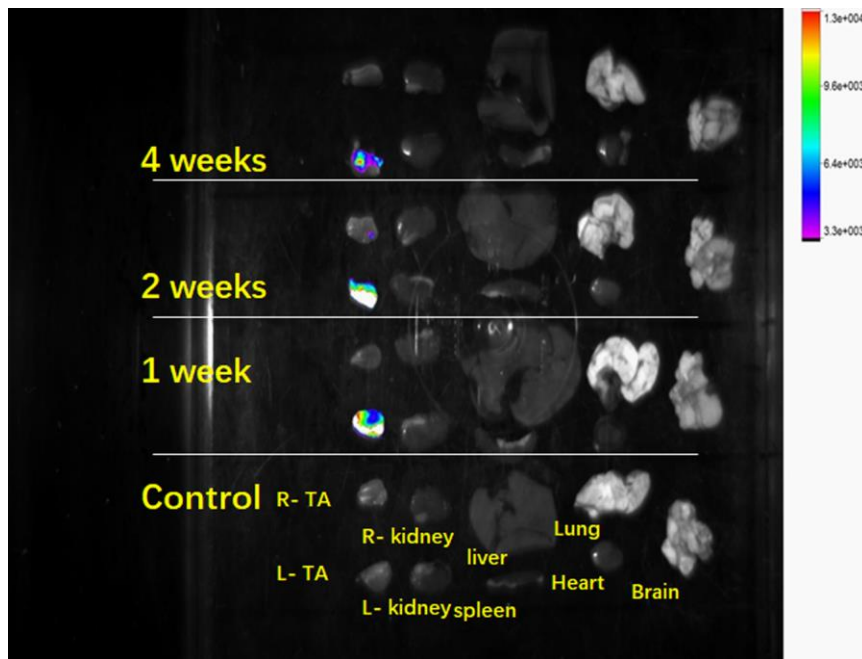


Figure S9: injection of the DiR only into the left TA muscle did not result in multiple organ distribution

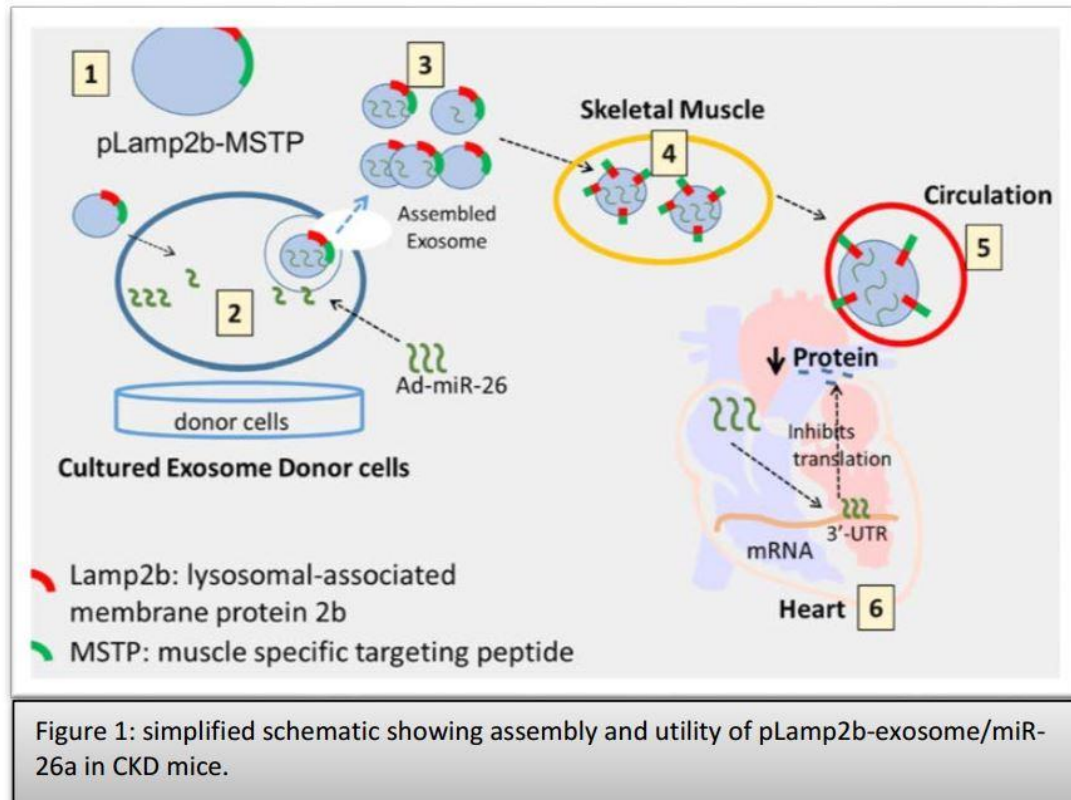
The fluorescence distribution was determined in muscle and organs at 1, 2 and 4 weeks after intramuscular injection of DiR without exosome and microRNA in normal mice. Each organ was removed from the mice that received intramuscular injection of DiR in the left TA muscle. Images were taken of each organs; the bottom mouse did not receive any DiR injection. Organs from right to left: brain, lung (top) and heart (bottom), liver (top) and spleen (bottom), kidneys (top: right kidney and bottom: left kidney) and TA muscle (top: right muscle and bottom: left muscle).

A detailed, expanded Methods:

CKD mice model and treatment: The experiments were approved by the Emory University IACUC (protocol 4000152). Mice (C57BL/6J) from Jackson Laboratories (Bar Harbor, ME, USA) were kept in a 12-hour light/12-hour dark cycle. Under anesthesia (pentobarbital), CKD model was obtained through a two-steps of 5/6 nephrectomy. At the first week we removed 2/3 of the left kidney, after one week recovery, we removed the right side kidney. After 2nd surgery, CKD mice were fed 14% protein rodent maintenance diet chow (Harlan Teklad, Madison, WI, USA) ad

libitum for 7 days before sham-operated mice were weight-matched with a CKD mouse and pair-fed a 14% protein diet for 2 weeks and 40% protein diet for 5 weeks. We started Exo/*miR-26a* or Exo/control tibialis anterior (TA) injection after second CKD surgery, 40 ug exosomes each time, once per week total 8 weeks. All mice were feed with 0.9% salts water from the 2nd week. CKD mice with blood urea nitrogen (BUN) ~100 mg/dl (Roche Diagnostics Corporation, IN, USA) were studied.

Generation of exosome encapsulated *miR-26a*: We created a vector which produces *Lamp2b* (*lysosomal-associated membrane protein 2b*) fused with the Muscle specific surface peptide (*KKEEE*)_{3K} (#1 in Figure 1). Satellite cells were grown to 60% confluence in DMEM/F12 culture medium containing 20% fetal bovine serum. The *Lamp2b-MSTP* vector was transfected into satellite cells (#2 in Figure 1) using the Effectene transfection reagent (Qiagen, Valencia, CA, USA). Six hours after transfection, the cells were transduced with Ad-*miR-26a* (adenovirus containing *miR-26a* processor sequences) to produce exosome encapsulated *miR-26a* (Exo/*miR-26a*) [1]. Control cells were transduced with Ad-empty for production of *MSTP*-exosome-control (Exo/ctrl). Exosome-free medium was used to replace the growth medium to allow exosome secretion for 48 hours. Last, the *pLamp2b/MSTP-miR-26a* enriched exosomes (Exo/*miR-26a*) and *pLamp2b/MSTP-ctrl* exosomes (Exo/ctrl) were isolated from the conditioned medium of cultured cells and re-suspended in PBS (#3 in Figure 1).



Exosome purification, analysis, and modifying: Exosomes were purified by several centrifugation and filtration steps as described previously [2]. Briefly, the supernatant was centrifuged at 2,000 g for 10 minutes, and 16,000 g for 30 minutes, followed by filtration through a 0.22- μ m filter to eliminate cells and cellular debris. The supernatant was ultra-centrifuged at 160,000 g for 180 minutes (Ultracentrifuge, Beckman Coulter, L8-70M). The exosomes pellets were re-suspended in PBS and stored at -80°C . Exosomes were analyzed by NanoSight instrument measurement (Figure S2) and the presence of the exosomal marker protein TSG101 by western blot (Figure S3). we injected the exosome/miR into skeletal muscle of CKD mice (#4 in Figure 1). Muscle releases Exo/miR into the circulation (#5 in Figure 1). Because Lamp2b is ubiquitously expressed on the surface of exosomes, it can bring the targeting peptides (e.g. (KKEEE)3K) to the exosomes surface and endow exosome-encapsulated cargo (e.g. *miR-26*) with targeting ability (#6 in Figure 1).

Real time Quantitative PCR (qPCR): To measure microRNA, total RNA was extracted using Tri-Reagent (Molecular Research Inc., Cincinnati, OH). For synthesis cDNA, 10ng of total RNA that was enriched in small RNAs was reverse transcribed

using the NCode miRNA cDNA synthesis kit (Exiqon, Vedbaek, Denmark). The expression of pri-miR and pre-miR was measured as described [3]. PCR was used the cycle parameters: 94 °C for 2minutes and 45 cycles at 95 °C for 15 seconds and 60 °C for 60 seconds. The Ct (threshold cycle) was defined as the number of cycles required for the fluorescence signal to exceed the detection threshold. Primers were purchased from Exiqon. Expression of individual miRNA was standardized to the mouse U6 gene (tissue) or *miR-103a* (serum), and calculated as the difference between the threshold values of the two genes ($\Delta\Delta\text{Cq}$) [4, 5]. Melting curve analyses were performed during real-time qPCR to analyze and verify the specificity of the reaction.

miRNA-Seq Library Preparation and Sequencing: Qualitative and quantitative analysis of the total RNA was performed using the Thermo Nanodrop 2000 and Agilent 2100 Bioanalyzer respectively. Small RNA libraries were prepared using the SeqMatic tailormix miRNA sample preparation kit (SeqMatic. Union City, CA, USA) as per manufacturer's instructions. Briefly, 100 ng of total RNA was used for library preparation. Small RNA's were ligated with Illumina compatible adapters and each sample was tagged with a unique barcode to allow multiplexing. The adapter-ligated libraries were then enriched using PCR amplification followed by gel enrichment for mature miRNA library. The amplified library was validated using a High Sensitivity DNA chip on the Agilent Bioanalyzer. The libraries were further quantified on Qubit® 2.0 Fluorometer (Life Technologies, Grand Island, NY, USA) using the High Sensitivity dsDNA assay. Libraries from all the samples were multiplexed and run in a single lane of Illumina 3K flowcell. PhiX was used as an internal control on each lane to monitor the error statistics. Cluster generation was performed on the v3 flowcell on the Illumina cBot. The clustered flowcell was sequenced on the Illumina HiSeq3000 system as a 100-cycle single read multiplexed run.

Primary muscle satellite cell culture: Satellite were isolated from hind-limb muscles of 4 months old mice as described. Dissociation of mouse skeletal muscle tissue into single-cell suspensions using Skeletal Muscle Dissociation Kit (130-098-305; MACS, Miltenyi Biotec, Inc. Auburn, CA, USA), Satellite Cell Isolation Kit (130-104-267, MACS, Miltenyi Biotec, Inc. Auburn, CA, USA) was

used to isolate muscle progenitor cells. Satellite cells were identified using anti-eMyHC (45). Anti- α -smooth muscle actin (Sigma-Aldrich, St. Louis, MO, USA) was used to identify fibroblast contamination and the positive cells are less than 1% [6]. Luciferase Reporter Assay and Transfection: The luciferase reporter constructs in which the luciferase coding sequence was fused to the 3'-UTRs of *FOXO1* (*pLuc.miR-26a/FoxO1-3'UTR*) was generated by the Emory Integrated Genomics Core (EIGC). For transfection, C2C12 cells in growth medium were seeded in 24-well plates and transfected using effectene transfection reagent (Qiagen, Valencia, CA, USA). In each well, 0.2 μ g of firefly luciferase vector and 0.04 μ g of the renilla luciferase (control vector) were introduced. After 24 hours, the renilla luciferase activities were measured consecutively by dual-luciferase assays (Promega, Madison, WI, USA) using TD-20/20 Luminometer (Turner Designs, Sunnyvale, CA, USA) [7]. We calculated the results as the ratio of firefly luciferase to renilla luciferase ($\times 100$). Results from control experiments (e.g, *pLuc-3UTR-FOXO1* expressing cells that were treated with a control adenovirus) are expressed as 100%. Experimental results were calculated in the same fashion and expressed as a percent of control levels.

Masson staining and immunofluorescence staining: Heart sections (3 μ m thick) stained with Masson staining to evaluate heart fibrosis. Indirect immunofluorescence staining was performed according to an established procedure. Briefly, the cells were fixed with cold acetone for 10 min, and frozen sections of TA tissues (5 μ m thickness) were prepared. After being blocked with 3% bovine serum albumin (BSA) for 1 h, the cells and sections were incubated overnight at 4°C with primary antibodies against laminin (1:200) and Fibronectin (1:200) in PBS containing 3% BSA. Sections were then washed with PBS and incubated in the dark with tetramethylrhodamine isothiocyanate (TRITC)- conjugated secondary antibodies (Sigma-Aldrich, St. Louis, MO, USA) at a 1:200 dilution in PBS containing 3% BSA for 1 h. After being thoroughly washed with PBS, slides were mounted with 4',6-diamidino-2-phenylindole (DAPI, H-1200, Vector Laboratories, Burlingame, CA, USA) and viewed with a Nikon Eclipse 80i Epi-fluorescence microscope equipped

with a digital camera (DS-Ri1, Nikon, Tokyo, Japan). The above histological analysis was performed in a blind manner to avoid bias. All immunohistochemical analyses were repeated at least three times, and representative images are shown.

Western blot analysis: Satellite and H9C2 cells harvested from plates and heart and TA tissues were lysed in RIPA buffer. Detection of protein expression by western blot was performed according to established protocols. Equal amounts of protein were subjected to SDS- polyacrylamide gel electrophoresis (PAGE) on 10 to 12% polyacrylamide gels and transferred to a polyvinylidene difluoride membrane (HATF09025, Millipore, Burlington, MA, USA). The membrane with blotted protein was blocked for 1 h with blocking buffer containing 5% nonfat dry milk and 0.05% Tween-20 in Tris-buffered saline (TBS-T), followed by incubation with the primary antibodies as follows: Primary antibodies (1:1000 dilution except indicated): Akt(C67E7), p-Akt Ser473(D9E), FoxO1(75D8), pFoxO1(Thr24, #9464), CTGF(1:200), GSK-3 β (D5C5Z) and phospho-GSK-3 α/β (Ser21/9) were from Cell Signaling (Danvers, MA, USA). Type I collagen (Cat# 131001; Southern Biotech, Birmingham, AL, USA), PTEN (Cat# FL-403) were from Santa Cruz (Santa Cruz, CA, USA); GAPDH (1: 5000 dilution, Cat# MAB374) was from Millipore (Burlington, MA, USA). COL4A1 (ab6586), TRIM63/MuRF1 (ab77577) and FBXO32/atrogen-1 (ab168372) were from Abcam (Cambridge, MA, USA); fibronectin and (F3648) were from Sigma-Aldrich (St. Louis, MO, USA). CTGF (SC-149390) was from Santa Cruz (Santa Cruz, CA, USA). The bands were detected using the ChemiDoc XRS System (Bio-Rad, Hercules, CA, USA). The relative intensity of each band was normalized to GAPDH.

Virus Reagents: The Ad-*miR-26a* and control virus (Ad-empty) were produced by Emory Integrated Genomics Core. The adenovirus transduction unit (TU) was achieved by serial dilutions, and 5 μ l of the concentrated viral preparation (109 TU) was added to 2ml media and applied to 6well plates; 90% of cells were transduced (based on green fluorescent protein expression). We used the Ad-*miR-26a* adenovirus to express *miR-26a*. Adenovirus transduction was accomplished when growth media was changed to differentiation media.

Echocardiographic Evaluations of Cardiac Function: Echocardiography was performed on lightly anesthetized mice (under 1-2% isoflurane, in oxygen) using a Vevo 3,100 ultrasound system (VisualSonics, Toronto, CA) as described previously [8]. LV dimensions were obtained from parasternal long-axis long axis views by two-dimensional-guided M-mode imaging, cursor was positioned perpendicular to the interventricular septum and posterior wall of the LV at the level of the papillary muscles and an M-mode image was obtained at a sweep speed of 100 mm/s and used to determine diastolic and systolic LV wall thickness, LV end-diastolic dimensions (LVDD) and LV end-systolic chamber dimensions (LVSD). Systolic function was calculated from LV dimensions as fractional shortening (FS), as follows: $FS = (LVDD - LVSD) / LVDD$. Recording of echocardiographic images was performed in random order with respect to the treatment or control animals. The acquisition of images and evaluation of data were performed by independent operator, who were blinded to the treatment.

Statistical analysis: Data were presented as mean \pm se. To identify significant differences between two groups, comparisons were made by using the t-test. Differences with P values < 0.05 were considered significant. For a comparison of more than two groups, one-way ANOVA was performed with a post hoc analysis by the StudentNewman-Keuls test. Differences with P values < 0.05 were considered significant.

Reference:

1. Wang XH, Hu Z, Klein JD, Zhang L, Fang F, Mitch WE. Decreased miR-29 suppresses myogenesis in CKD. *J Am Soc Nephrol.* 2011; 22: 2068-76.
2. Wang B, Zhang C, Zhang A, Cai H, Price SR, Wang XH. MicroRNA-23a and MicroRNA-27a Mimic Exercise by Ameliorating CKD-Induced Muscle Atrophy. *J Am Soc Nephrol.* 2017; 28: 2631-40.
3. Su Z, Hu L, Cheng J, Klein JD, Hassounah F, Cai H, et al. Acupuncture plus low-frequency electrical stimulation (Acu-LFES) attenuates denervation-induced muscle atrophy. *J Appl Physiol (1985).* 2016; 120: 426-36.

4. Hu L, Klein JD, Hassounah F, Cai H, Zhang C, Xu P, et al. Low-frequency electrical stimulation attenuates muscle atrophy in CKD--a potential treatment strategy. *J Am Soc Nephrol.* 2015; 26: 626-35.
5. Su Z, Klein JD, Du J, Franch HA, Zhang L, Hassounah F, Hudson MB, Wang XH. Chronic kidney disease induces autophagy leading to dysfunction of mitochondria in skeletal muscle. *Am J Physiol Renal Physiol.* 2017; 312: F1128-40.
6. Du J, Klein JD, Hassounah F, Zhang J, Zhang C, Wang XH. Aging increases CCN1 expression leading to muscle senescence. *Am J Physiol Cell Physiol.* 2014; 306: C28-36.
7. Wang X, Chinsky JM, Costeas PA, Price SR. Acidification and glucocorticoids independently regulate branched-chain alpha-ketoacid dehydrogenase subunit genes. *Am J Physiol Cell Physiol.* 2001; 280: C1176-83.
8. Naqvi N, Li M, Calvert JW, Tejada T, Lambert JP, Wu J, et al. A proliferative burst during preadolescence establishes the final cardiomyocyte number. *Cell.* 2014; 157: 795-807.